Journal of Sound and Vibration (2000) **234**(3), 369–386
doi:10.1006/jsvi.1999.2881, available online at http://www.idealibrary.com on IDEAL®

VIBRATION OF STRAIGHT–CURVED–STRAIGHT HOLLOW SHAFTS

RONG-TYAI WANG

National Cheng Kung University, Tainan, Taiwan, 701, Republic of China

(*Received* 21 *April* 1999, *in final form* 4 *October* 1999)

This work presents the governing equations for both the in-plane motion and out-of-plane motion of a curved hollow shaft. Two types of shaft structures, which are a curved hollow shaft and a straight–curved–straight hollow shaft, are considered. An analytical method is also presented to examine the free vibration of the two types of shaft structures. The orthogonality of any two distinct sets of mode shape functions for both the in-plane motion and out-of-plane motion of the structures is also derived. The first in-plane modal frequency of a structure is greater than the first out-of-plane modal frequency of the same structure.

1. INTRODUCTION

The ducts with a circular cross-section have been widely used in fluid transportation. The duct structures can basically be simulated as hollow shafts. The displacement fields of a hollow shaft contain three displacement components, two bending slopes and one twist angle. Hollow shaft structures are normally organized in a straight type. Owing to the restriction of space and environment, hollow shafts are almost arranged in a straight–curved–straight type for industrial usage. The geometry of this type of shaft structure completely differs from that of a straight shaft. The initial curvature of a curved hollow shaft causes the coupling effect between twist angle and bending slope in bending moment and torque. The coupling effect causes the governing equations of curved hollow shafts to be more complicated than those of straight hollow shafts.

The straight–curved–straight hollow shaft consists of two straight hollow shafts and one curved hollow shaft. The vibration of this type of shaft structure induced by external forces sometimes causes significant disasters. However, the vibration problems of this type of shaft structure have rarely been studied. The hollow shaft can basically be regarded as a hollow beam. There are two kinds of motions for the hollow beam: in-plane motion and out-of-plane motion. The vibration of straight beams can be easily examined based on the Timoshenko beam theory. As for curved beams, the free vibration of the out-of-plane motion of the shafts has been studied over two decades [1–5]. Moreover, the vibration of thin-walled beam can be examined based on Vlasov's [6] theory. Wang and Sang [7] set up the displacements for a curved beam to derive the equations for the out-of-plane motion of the beam via the Timoshenko beam theory. Further, Wang [8] set up the displacements, which are three displacement components; two bending slopes and one twist angle, for a curved frame to derive the governing equations of a T-type curved frame via the same beam theory. Further, an analytical method has been successfully adopted in studying the forced vibration of a multi-span curved beam and the T-type curved frame due to a moving

0022-460X/00/280369 + 18 $35.00/0

force. Therefore, an analytical method will be proposed in the paper to study the vibration of straight–curved–straight hollow shaft structures.

The study presents the displacements of curved hollow shaft and those of a straight hollow shaft. The hollow shafts have a circular type of cross-section. Further, the shafts are considered to be homogeneous and isotropic with Young's modulus E, shear modulus G, Poisson's ratio μ and mass density ρ. The initial radius of the curved shaft is considered to be larger than the radius of the cross-section of the shaft. The governing equations for the in-plane motion of the curved hollow shaft and the straight hollow shafts are presented. A fixed–fixed curved hollow shaft and a fixed–fixed straight–curved–straight hollow shaft are taken as two examples. An analytical method is presented to obtain the respective frequency responses for the in-plane motion and the out-of-plane motion and the out-of-plane motion of the hollow shaft structures. The transfer matrix of response relations between two ends of each shaft component is set up. The modal frequencies and their corresponding sets of mode shape functions for either the in-plane motion or the out-of-plane motion of the two types of hollow shaft structures are obtained via the method of transfer matrix. Further, the orthogonality of any two distinct sets of mode shape functions for either the in-plane motion or the out-of-plane motion is derived to quarantee the feasibility of the method of modal analysis. The effects of initial radius and thickness and radius of cross-section of the curved hollow shaft on the modal frequencies of the two shaft structures are investigated.

2. STRESS RESULTANTS

2.1. CURVED HOLLOW SHAFT

A curved hollow shaft is depicted in Figure 1(a). The angle measured from the bisector of angle between any ends is φ. The radius of the shaft along its curved axes is R. The Cartesian co-ordinates (x, y and z) system and the cylindrical co-ordinate (r, θ and z) system for the shaft are depicted in the figure. The x- and z-axis coincide with the principal centrodial axes of the shaft, while the y-axis is tangent to the curved axis of the shaft. The co-ordinates r, θ and z are taken at the center of curvature of the shaft. The shaft has a uniformly circular cross-section with radius a and thickness h. The displacement components along these principal axes are denoted as u_x, u_y and u_z respectively. Furthermore, ϕ_x, ϕ_y and ϕ_z are the respective rotation angles of the cross-section along these principal axes.

The displacement fields of the cross-section along these principal axes in the Cartesian co-ordinates are

$$u_{x^*}(x, y, z, t) = u_x(y, t) + z\phi_y(y, t), \tag{1a}$$

$$u_{y^*}(x, y, z, t) = u_y(y, t) - z\phi_x(y, t) + x\phi_z(y, t), \tag{1b}$$

$$u_{z^*}(x, y, z, t) = u_z(y, t) - x\phi_y(y, t). \tag{1c}$$

By performing similar procedures described by Wang [8], the stress resultants q_x, $q_y(= q_\theta)$ and q_z, and the stress-couple resultants m_x, $m_y(= m_\theta)$ and m_z of the curved shaft about the principal axes are obtained:

$$q_x = \kappa GA\left(\frac{\partial u_x}{\partial y} - \frac{u_y}{R} + \phi_z\right), \quad q_y = q_\theta = EA\left(\frac{\partial u_y}{\partial y} + \frac{u_x}{R}\right), \tag{2a, b}$$

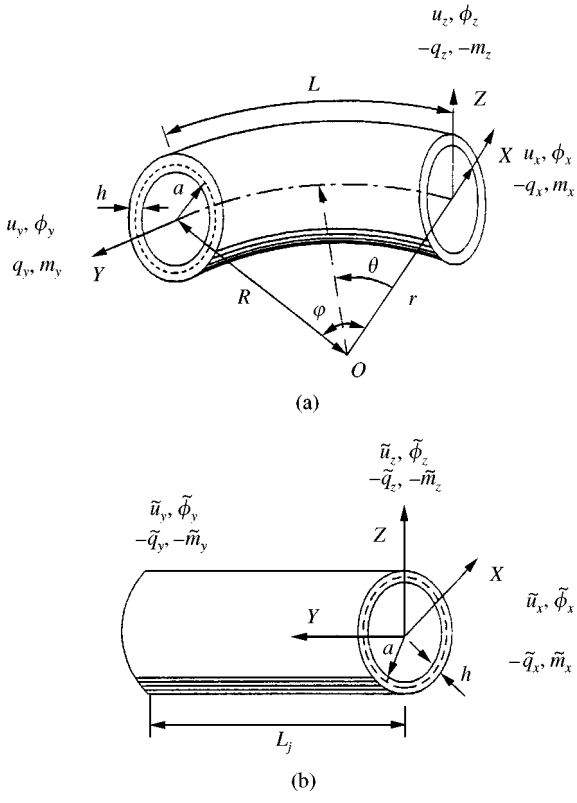

Figure 1. Displacements, stress resultants and stress-couple resultants for (a) the curved hollow shaft and (b) the straight hollow shaft.

$$q_z = \kappa GA\left(\frac{\partial u_z}{\partial y} - \phi_x\right), \quad m_x = m_r = -EI\left(\frac{\partial \phi_x}{\partial y} - \frac{\phi_y}{R}\right), \tag{2c, d}$$

$$m_y = m_\theta = GJ\left(\frac{\partial \phi_y}{\partial y} + \frac{\phi_x}{R}\right), \quad m_z = EI\frac{\partial \phi_z}{\partial y}, \tag{2e, f}$$

where A is the cross-sectional area, J is the polar moment of the cross-section and I is the moment of area about the x-axis or the z-axis.

2.2. STRAIGHT HOLLOW SHAFT

The Cartesian co-ordinate (x, y and z) system of the straight hollow shaft is depicted in Figure 1(b). The x- and z-axis coincide with the principal centroidal axes of the shaft while the y-axis denotes the longitudinal axis of the shaft. The shaft has a uniform circular cross-section with radius a and thickness h, polar moment J around the y-axis, and second moment of area I around the x-axis (or z-axis). The displacement components along these principal axes are denoted as $\tilde{u}_x$, $\tilde{u}_y$ and $\tilde{u}_z$ respectively. Furthermore, $\tilde{\phi}_x$, $\tilde{\phi}_y$ and $\tilde{\phi}_z$ are the respective rotation angles of the cross-section along these principal axes. The displacement

fields of the cross-section along these principal axes in the Cartesian co-ordinates are

$$\tilde{u}_{x*}(x, y, z, t) = \tilde{u}_x(y, t) + z\tilde{\phi}_y(y, t), \tag{3a}$$

$$\tilde{u}_{y*}(x, y, z, t) = \tilde{u}_y(y, t) - z\tilde{\phi}_x(y, t) + x\tilde{\phi}_z(y, t), \tag{3b}$$

$$\tilde{u}_{z*}(x, y, z, t) = \tilde{u}_z(y, t) - x\tilde{\phi}_y(y, t). \tag{3c}$$

The stress resultants $\tilde{q}_x$, $\tilde{q}_y$ and $\tilde{q}_z$, and the stress-couple resultants $\tilde{m}_x$, $\tilde{m}_y$ and $\tilde{m}_z$ of the shaft along these principal axes are

$$\tilde{q}_x = \kappa GA\left(\frac{\partial \tilde{u}_x}{\partial y} + \tilde{\phi}_z\right), \quad \tilde{q}_y = EA\frac{\partial \tilde{u}_y}{\partial y}, \quad \tilde{q}_z = \kappa GA\left(\frac{\partial \tilde{u}_z}{\partial y} - \tilde{\phi}_x\right), \tag{4a–c}$$

$$\tilde{m}_x = -EI\frac{\partial \tilde{\phi}_x}{\partial y}, \quad \tilde{m}_y = GJ\frac{\partial \tilde{\phi}_y}{\partial y}, \quad \tilde{m}_z = EI\frac{\partial \tilde{\phi}_z}{\partial y} \tag{4d–f}$$

3. EQUATIONS OF MOTION

3.1. CURVED HOLLOW SHAFT

The governing equations for the in-plane motion of the curved hollow shaft are [8]

$$-\frac{\partial q_x}{\partial y} + \frac{q_y}{R} + \rho A\frac{\partial^2 u_x}{\partial t^2} = 0, \quad -\frac{q_x}{R} - \frac{\partial q_y}{\partial y} + \rho A\frac{\partial^2 u_y}{\partial t^2} = 0,$$

$$q_x - \frac{\partial m_z}{\partial y} + \rho I\frac{\partial^2 \phi_z}{\partial t^2} = 0. \tag{5a–c}$$

Further, the governing equations for the out-of-plane motion of the shaft are

$$-\frac{\partial q_z}{\partial y} + \rho A\frac{\partial^2 u_z}{\partial t^2} = 0, \quad -q_z + \frac{m_y}{R} + \frac{\partial m_x}{\partial y} + \rho I\frac{\partial^2 \phi_x}{\partial t^2} = 0,$$

$$-\frac{\partial m_y}{\partial y} + \frac{m_x}{R} + \rho J\frac{\partial^2 \phi_y}{\partial t^2} = 0. \tag{6a–c}$$

The sign conventions for the displacements, rotations, stress resultants and stress-couple resultants at the two ends of the curved hollow shaft are

$$\{d_{r1}\}(t) = \{u_x u_y \phi_z\}^{\mathrm{T}}(0, t), \quad \{f_{r1}\}(t) = \{-q_x - q_y - m_z\}^{\mathrm{T}}(0, t), \tag{7a, b}$$

$$\{d_{l1}\}(t) = \{u_x u_y \phi_z\}^{\mathrm{T}}(L, t), \quad \{f_{r1}\}(t) = \{q_x q_y m_z\}^{\mathrm{T}}(L, t), \tag{7c, d}$$

$$\{d_{r2}\}(t) = \{u_z \phi_x \phi_y\}^{\mathrm{T}}(0, t), \quad \{f_{r2}\}(t) = \{-q_z m_x - m_y\}^{\mathrm{T}}(0, t), \tag{8a, b}$$

$$\{d_{l2}\}(t) = \{u_z \phi_x \phi_y\}^{\mathrm{T}}(L, t), \{f_{l2}\}(t) = \{q_z - m_x m_y\}^{\mathrm{T}}(L, t). \tag{8c, d}$$

3.2. STRAIGHT HOLLOW SHAFTS

The governing equations for the in-plane motion and the out-of-plane motion of one straight hollow shaft can be obtained similarly as

$$-\frac{\partial \tilde{q}_x}{\partial y}+\rho A\frac{\partial^2 \tilde{u}_x}{\partial t^2}=0,\quad -\frac{\partial \tilde{q}_y}{\partial y}+\rho A\frac{\partial^2 \tilde{u}_y}{\partial t^2}=0,\quad \tilde{q}_x=\frac{\partial \tilde{m}_z}{\partial y}+\rho I\frac{\partial^2 \tilde{\phi}_z}{\partial t^2}=0, \tag{9a–c}$$

$$-\frac{\partial \tilde{q}_z}{\partial y}+\rho A\frac{\partial^2 \tilde{u}_z}{\partial t^2}=0,\quad -\tilde{q}_z+\frac{\partial \tilde{m}_x}{\partial y}+\rho I\frac{\partial^2 \tilde{\phi}_x}{\partial t^2}=0,\quad -\frac{\partial \tilde{m}_y}{\partial y}+\rho J\frac{\partial^2 \tilde{\phi}_y}{\partial t^2}=0. \tag{10a–c}$$

The sign conventions for the displacements, rotations, stress resultants and stress-couple resultants at the two ends of the jth straight hollow shaft are

$$\{\tilde{d}_{r1}\}_J(t)=\{\tilde{u}_x\tilde{u}_y\tilde{\phi}_z\}_j^{\mathrm{T}}(0,t),\ \{\tilde{f}_{r1}\}_j(t)=\{-\tilde{q}_x-\tilde{q}_y-\tilde{m}_z\}_j^{\mathrm{T}}(0,t), \tag{11a, b}$$

$$\{\tilde{d}_{r1}\}_j(t)=\{\tilde{u}_x\tilde{u}_y\tilde{\phi}_z\}_j^{\mathrm{T}}(L_j,t),\quad \{\tilde{f}_{l1}\}_j(t)=\{\tilde{q}_x\tilde{q}_y\tilde{m}_z\}_j^{\mathrm{T}}(L_j,t), \tag{11c, d}$$

$$\{\tilde{d}_{r2}\}_j(t)=\{\tilde{u}_z\tilde{\phi}_x\tilde{\phi}_y\}_j^{\mathrm{T}}(0,t),\ \{\tilde{f}_{r2}\}_j(t)=\{-\tilde{q}_z\tilde{m}_x-\tilde{m}_y\}_j^{\mathrm{T}}(0,t), \tag{12a, b}$$

$$\{\tilde{d}_{l2}\}_j(t)=\{\tilde{u}_z\tilde{\phi}_x\tilde{\phi}_y\}_j^{\mathrm{T}}(L_j,t),\ \{\tilde{f}_{l2}\}_j(t)=\{\tilde{q}_z-\tilde{m}_x\tilde{m}_y\}_j^{\mathrm{T}}(L_j,t),\quad j=1,2, \tag{12c, d}$$

where L_j is the length of the shaft.

3.3. BOUNDARY CONDITIONS

3.3.1. *Fixed–fixed curved hollow shaft*

The boundary conditions at the two ends of a fixed–fixed curved hollow shaft (see Figure 2(a)) are

$$\{d_{r1}\}(t)=\{d_{r2}\}(t)=\{d_{l1}\}(t)=\{d_{l2}\}(t)=\{0\ 0\ 0\}^{\mathrm{T}} \tag{13}$$

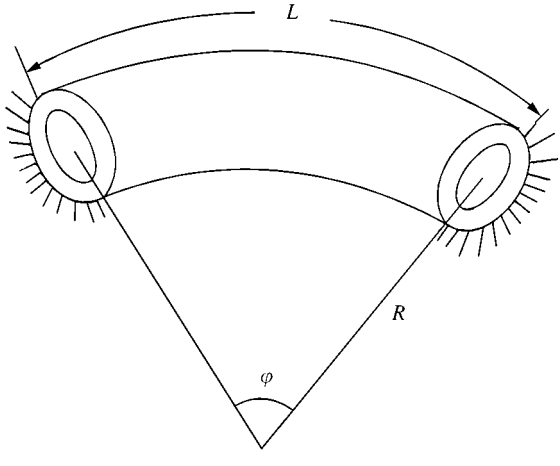

Figure 2. A fixed–fixed curved hollow shaft.

3.3.2. *Fixed–fixed straight–curved–straight hollow shaft*

The boundary conditions at the two ends of a fixed–fixed straight–curved–straight hollow shaft (see Figure 2(b)) are

$$\{\tilde{d}_{r1}\}_1(t) = \{\tilde{d}_{l1}\}_2(t) = \{0\ 0\ 0\}^{\mathrm{T}}, \{\tilde{d}_{r2}\}_1(t) = \{\tilde{d}_{l2}\}_2(t) = \{0\ 0\ 0\}^{\mathrm{T}}. \tag{14a, b}$$

Further, the displacement continuity and the force balances at two balances at two connections between the curved shaft and the two straight shafts respectively, are

$$\{d_{r1}\}(t) = \{\tilde{d}_{l1}\}_1(t), \{f_{r1}\}(t) = -\{\tilde{f}_{l1}\}_1(t), \tag{15a, b}$$

$$\{d_{r2}\}(t) = \{\tilde{d}_{l2}\}_1(t), \{f_{r2}\}(t) = -\{\tilde{f}_{l2}\}_1(t), \tag{15c, d}$$

$$\{d_{l1}\}(t) = \{\tilde{d}_{r1}\}_2(t), \{f_{l1}\}(t) = -\{\tilde{f}_{r1}\}_2(t), \tag{16a, b}$$

$$\{d_{l2}\}(t) = \{\tilde{d}_{r2}\}_2(t), \{f_{l2}\}(t) = -\{\tilde{f}_{r2}\}_2(t). \tag{16c, d}$$

4. FREQUENCY RESPONSES

4.1. IN-PLANE MOTION OF CURVED HOLLOW SHAFT

The responses u_x, u_y, ϕ_z, q_x, q_z and m_z for the in-plane motion of curved hollow shaft are denoted as

$$(u_x u_y \phi_z q_x q_y m_z)(y, t) = (U_x U_y \Phi_z Q_x Q_y M_z)(y) \sin(\omega t), \tag{17}$$

where

$$Q_x = \kappa GA\left(\frac{\mathrm{d}U_x}{\mathrm{d}y} - \frac{U_y}{R} + \Phi_z\right), \quad Q_y = EA\left(\frac{\mathrm{d}U_y}{\mathrm{d}y} + \frac{U_x}{R}\right), \quad M_z = EI\frac{\mathrm{d}\Phi_z}{\mathrm{d}y}, \tag{18a–c}$$

in which ω denotes the circular frequency. Substituting equations (17)–(18c) into equations (5a)–(5c) yields

$$-\frac{\mathrm{d}Q_x}{\mathrm{d}y} + \frac{Q_y}{R} = \rho A\omega^2 U_x, \quad -\frac{Q_x}{R} - \frac{\mathrm{d}Q_y}{\mathrm{d}y} = \rho A\omega^2 U_y,$$

$$Q_x - \frac{\mathrm{d}M_z}{\mathrm{d}y} = \rho I\omega^2 \Phi_z. \tag{19a–c}$$

The solutions of equations (19a)–(19c) are [8]

$$\{U_x U_y \Phi_z\}^{\mathrm{T}}(y) = \sum_{i=1}^{6} a_i \{p_i g_i p_i^*\}^{\mathrm{T}}(y), \tag{20a}$$

$$\{Q_x Q_y M_z\}^{\mathrm{T}}(y) = \sum_{i=1}^{6} a_i \{\eta_i \beta_i \zeta_i\}^{\mathrm{T}}(y), \tag{20b}$$

where a_1–a_6 are constants needed to be determined.

The sign conventions for the frequency responses of the displacements, rotation, stress resultants and stress-couple resultants at the two ends of the curved shaft can be expressed as

$$\{d_{r1}\}(t) = \{D_{r1}\}\sin(\omega t), \quad \{f_{r1}\}(t) = \{F_{r1}\}\sin(\omega t\}, \tag{21a, b}$$

$$\{d_{l1}\}(t) = \{D_{l1}\}\sin(\omega t), \quad \{f_{l1}\}(t) = \{F_{l1}\}\sin(\omega t). \tag{21c, d}$$

where

$$\{D_{r1}\} = \{U_x Y_y \Phi_z\}^{\mathrm{T}}(0), \{F_{r1}\} = \{-Q_x - Q_y - M_z\}^{\mathrm{T}}(0), \tag{22a, b}$$

$$\{D_{l1}\} = \{U_x Y_y \Phi_z\}^{\mathrm{T}}(L), \{F_{l1}\} = \{Q_x Q_y M_z\}^{\mathrm{T}}(L), \tag{22c, d}$$

Substituting equations (20a) and (20b) into equations (22a) and (22b) simultaneously and solving the constants a_1–a_6 in terms of $\{D_{r1}\}$ and $\{F_{r1}\}$, then substituting these values of a_1–a_6 into equations (22c) and (22d) and arranging the results into the symbolic vector form yields

$$\begin{Bmatrix} D_{l1} \\ F_{l1} \end{Bmatrix} = \begin{bmatrix} B_{11} & B_{12} \\ B_{21} & B_{22} \end{bmatrix} \begin{Bmatrix} D_{r1} \\ F_{r1} \end{Bmatrix}. \tag{23}$$

Equation (23) presents the relation of in-plane frequency responses at the two ends of the curved shaft.

4.2. OUT-OF-PLANE MOTION OF CURVED HOLLOW SHAFT

The responses u_z, ϕ_x, ϕ_y, q_z, m_x and m_y for the out-of-plane motion of the curved hollow shaft are denoted as

$$(u_z \phi_x \phi_y q_z m_x m_v)(y, t) = (U_z \Phi_x \Phi_y Q_z M_x M_y)(y)\sin(\omega t), \tag{24}$$

where

$$Q_z = \kappa GA\left(\frac{\mathrm{d}U_z}{\mathrm{d}y} - \Phi_x\right), \quad M_x = -EI\left(\frac{\mathrm{d}\Phi_x}{\mathrm{d}y} - \frac{\Phi_y}{R}\right), \quad M_y = GJ\left(\frac{\mathrm{d}\Phi_y}{\mathrm{d}y} + \frac{\Phi_x}{R}\right), \tag{25a–c}$$

in which ω denotes the circular frequency. Substituting equations (24)–(25c) into equations (6a)–(6c) yields

$$-\frac{\mathrm{d}Q_z}{\mathrm{d}y} = \rho A\omega^2 U_z, \quad -Q_z + \frac{M_y}{R} + \frac{\mathrm{d}M_x}{\mathrm{d}y} = \rho I\omega^2 \Phi_x,$$

$$-\frac{\mathrm{d}M_y}{\mathrm{d}y} + \frac{M_x}{R} = \rho J\omega^2 \Phi_y. \tag{26a–c}$$

The solutions of equations (26a)–(26c) are [7]

$$\{U_z\Phi_x\Phi_y\}^{\mathrm{T}}(y) = \sum_{i=7}^{12} a_i\{p_i g_i p_i^*\}^{\mathrm{T}}(y), \tag{27a}$$

$$\{Q_z M_x M_y\}^{\mathrm{T}}(y) = \sum_{i=7}^{12} a_i\{\eta_i\beta_i\zeta_i\}^{\mathrm{T}}(y), \tag{27b}$$

where a_7–a_{12} are constants needed to be determined.

By performing similar procedures described in the preceding section, the relation of out-of-plane frequency responses at the two ends of the shaft can be expressed in the symbolic form as

$$\begin{Bmatrix} D_{l2} \\ F_{l2} \end{Bmatrix} = \begin{bmatrix} C_{11} & C_{12} \\ C_{21} & C_{22} \end{bmatrix} \begin{Bmatrix} D_{r2} \\ F_{r2} \end{Bmatrix}, \tag{28}$$

where

$$\{D_{r2}\} = \{U_z\Phi_x\Phi_y\}^{\mathrm{T}}(0), \{F_{r2}\} = \{-Q_z M_x - M_y\}^{\mathrm{T}}(0), \tag{29a, b}$$

$$\{D_{l2}\} = \{U_z\Phi_x\Phi_y\}^{\mathrm{T}}(L), \{F_{l2}\} = \{Q_z - M_x M_y\}^{\mathrm{T}}(L). \tag{29c, d}$$

4.3. STRAIGHT HOLLOW SHAFT

The responses $\tilde{u}_{xj}, \tilde{u}_{yj}, \tilde{u}_{zj}, \tilde{\phi}_{xj}, \tilde{\phi}_{yj}, \tilde{\phi}_{zj}, \tilde{q}_{xj}, \tilde{q}_{yj}, \tilde{q}_{zj}, \tilde{m}_{xj}, \tilde{m}_{yj}$ and $\tilde{m}_{zj}$ of the jth straight shaft are denoted as

$$(\tilde{u}_x\tilde{u}_y\tilde{\phi}_z\tilde{q}_x\tilde{q}_v\tilde{m}_z)_j(y, t) = (\tilde{U}_x\tilde{U}_y\tilde{\Phi}_z\tilde{Q}_z\tilde{Q}_x\tilde{M}_z)_j(y)\sin(\omega t), \tag{30a}$$

$$(\tilde{u}_z\tilde{\phi}_x\tilde{\phi}_v\tilde{q}_z\tilde{m}_x\tilde{m}_y)_j(y, t) = (\tilde{U}_z\tilde{\Phi}_x\tilde{\Phi}_y\tilde{Q}_z\tilde{M}_x\tilde{M}_y)_j(y)\sin(\omega t), \tag{30b}$$

where

$$\tilde{Q}_{xj} = \kappa GA\left(\frac{\mathrm{d}\tilde{U}_{xj}}{\mathrm{d}y} + \Phi_{zj}\right), \quad \tilde{Q}_{yj} = EA\frac{\mathrm{d}\tilde{U}_{yj}}{\mathrm{d}y}, \quad \tilde{Q}_{zj} = \kappa GA\left(\frac{\mathrm{d}\tilde{U}_{zj}}{\mathrm{d}y} - \tilde{\Phi}_{xj}\right), \tag{31a–c}$$

$$\tilde{M}_{xj} = EI\frac{\mathrm{d}\tilde{\Phi}_{xj}}{\mathrm{d}y}, \quad \tilde{M}_{yj} = GJ\frac{\mathrm{d}\tilde{\Phi}_{yj}}{\mathrm{d}y}, \quad \tilde{M}_{zj} = EI\frac{\mathrm{d}\tilde{\Phi}_{zj}}{\mathrm{d}y}, \tag{31d–f}$$

in which ω denotes the circular frequency. Under these circumstances, equations (9a)–(10c) becomes

$$-\frac{\mathrm{d}\tilde{Q}_{xj}}{\mathrm{d}y} = \rho A\omega^2\tilde{U}_{xj}, \; -\frac{\mathrm{d}\tilde{Q}_{yj}}{\mathrm{d}y} = \rho A\omega^2\tilde{U}_{yj}, \tag{32a, b}$$

$$-\frac{\mathrm{d}\tilde{Q}_{zj}}{\mathrm{d}y}=\rho A\omega^2\tilde{U}_{zj},\ -\tilde{Q}_{zj}+\frac{\mathrm{d}\tilde{M}_{xj}}{\mathrm{d}y}=\rho I\omega^2\tilde{\Phi}_{xj}, \tag{32c, d}$$

$$-\frac{\mathrm{d}\tilde{M}_{yj}}{\mathrm{d}y}=\rho J\omega^2\tilde{\Phi}_{yj},\ \tilde{Q}_{xj}-\frac{\mathrm{d}\tilde{M}_{zj}}{\mathrm{d}y}=\rho I\omega^2\tilde{\Phi}_{zj}. \tag{32e, f}$$

The general solutions of equations (32a)–(32f) can be expressed as

$$\{\tilde{U}_x\tilde{U}_y\tilde{\Phi}_z\}_j^{\mathrm{T}}(y)=\sum_{i=1}^{6}c_{ij}\{f_{1i}f_{2i}f_{3i}\}^{\mathrm{T}}(y), \tag{33a}$$

$$\{\tilde{Q}_x\tilde{Q}_y\tilde{M}_z\}_j^{\mathrm{T}}(y)=\sum_{i=1}^{6}c_{ij}\{f_{4i}f_{5i}f_{6i}\}^{\mathrm{T}}(y), \tag{33b}$$

$$\{\tilde{U}_z\tilde{\Phi}_x\tilde{\Phi}_y\}_j^{\mathrm{T}}(y)=\sum_{i=1}^{6}d_{ij}\{f_{1i}f_{3i}f_{7i}\}^{\mathrm{T}}(y), \tag{33c}$$

$$\{\tilde{Q}_z\tilde{M}_y\tilde{M}_x\}_j^{\mathrm{T}}(y)=\sum_{i=1}^{6}d_{ij}\{f_{4i}f_{8i}\ -f_{6i}\}^{\mathrm{T}}(y), \tag{33d}$$

where c_{1j}–c_{6j} and d_{1j}–d_{6j} denote constants and these functions $f_{11}(y)$–$f_{86}(y)$ are

$$f_{15}(y)=f_{16}(y)=0,\quad f_{21}(y)=f_{22}(y)=f_{23}(y)=f_{24}(y)=0.$$

$$f_{71}(y)=f_{72}(y)=f_{73}(y)=f_{74}(y)=0,$$

$$f_{25}(y)=\sin\left(\sqrt{\frac{\rho}{E}}\,\omega y\right),f_{26}(y)=\cos\left(\sqrt{\frac{\rho}{E}}\,\omega y\right),\quad f_{75}(y)=\sin\left(\sqrt{\frac{\rho}{G}}\,\omega y\right),$$

$$f_{76}(y)=\sin\left(\sqrt{\frac{\rho}{E}}\,\omega y\right),f_{3i}(y)=\frac{\mathrm{d}f_{1i}}{\mathrm{d}y}+\frac{\rho\omega^2}{\kappa G}\int f_{1i}\,\mathrm{d}y,\quad f_{4i}(y)=-\rho\omega^2A\int f_{1i}\,\mathrm{d}y,$$

$$f_{5i}(y)=EA\frac{\mathrm{d}f_{2i}}{\mathrm{d}y},\quad f_{6i}(y)=EI\frac{\mathrm{d}f_{3i}}{\mathrm{d}y},\quad f_{8i}(y)=GJ\frac{\mathrm{d}f_{7i}}{\mathrm{d}y}.$$

These functions $f_{11}(y)$–$f_{14}(y)$ are listed in Appendix A.

The sign conventions for the displacement, rotations, stress resultants and stress-couple resultants at the two ends of the straight shaft are

$$\{\tilde{d}_{r1}\}_j(t)=\{\tilde{D}_{r1}\}_j\sin(\omega t),\quad \{\tilde{f}_{r1}\}_j(t)=\{\tilde{F}_{r1}\}_j\sin(\omega t), \tag{34a, b}$$

$$\{\tilde{d}_{l1}\}_j(t)=\{\tilde{D}_{l1}\}_j\sin(\omega t),\quad \{\tilde{f}_{l1}\}_j(t)=\{\tilde{F}_{l1}\}_j\sin(\omega t), \tag{34c, d}$$

$$\{\tilde{d}_{r2}\}_j(t)=\{\tilde{D}_{r2}\}_j\sin(\omega t),\quad \{\tilde{f}_{r2}\}_j(t)=\{\tilde{F}_{r2}\}_j\sin(\omega t), \tag{34e, f}$$

$$\{\tilde{d}_{l2}\}_j(t)=\{\tilde{D}_{l2}\}_j\sin(\omega t),\quad \{\tilde{f}_{l2}\}_j(t)=\{\tilde{F}_{l2}\}_j\sin(\omega t), \tag{34g, h}$$

where

$$\{\tilde{D}_{r1}\}_j = \{\tilde{U}_x \tilde{U}_y \tilde{\Phi}_z\}_j^{\mathrm{T}}(0), \quad \{\tilde{F}_{r1}\}_j = \{-\tilde{Q}_x - \tilde{Q}_y - \tilde{M}_z\}_j^{\mathrm{T}}(0), \tag{35a, b}$$

$$\{\tilde{D}_{l1}\}_j = \{\tilde{U}_x \tilde{U}_y \tilde{\Phi}_z\}_j^{\mathrm{T}}(L_j), \quad \{\tilde{F}_{l1}\}_j = \{\tilde{Q}_x \tilde{Q}_y \tilde{M}_z\}_j^{\mathrm{T}}(L_j), \tag{35c, d}$$

$$\{\tilde{D}_{r2}\}_j = \{\tilde{U}_z \tilde{\Phi}_x \tilde{\Phi}_y\}_j^{\mathrm{T}}(0), \quad \{\tilde{F}_{r2}\}_j = \{-\tilde{Q}_z \tilde{M}_y - \tilde{M}_x\}_j^{\mathrm{T}}(0), \tag{35e, f}$$

$$\{\tilde{D}_{l2}\}_j = \{\tilde{U}_z \tilde{\Phi}_x \tilde{\Phi}_y\}_j^{\mathrm{T}}(L_j), \quad \{\tilde{F}_{l2}\}_j = \{\tilde{Q}_z - \tilde{M}_y \tilde{M}_x\}_j^{\mathrm{T}}(L_j). \tag{35g, h}$$

Substituting equations (33a) and (33b) into equations (35a) and (35b) simultaneously and solving the constants c_{1j}–c_{6j} in terms $\{\tilde{D}_{r1}\}_j$ and $\{\tilde{F}_{r1}\}_j$, then substituting these values of c_{1j}–c_{6j} into equations (35c) and (35d) and arranging the results into the symbolic vector form yields

$$\begin{Bmatrix} \tilde{D}_{l1} \\ \tilde{F}_{l1} \end{Bmatrix}_j = \begin{bmatrix} H_{11} & H_{12} \\ H_{21} & H_{22} \end{bmatrix}_j \begin{Bmatrix} \tilde{D}_{r1} \\ \tilde{F}_{r1} \end{Bmatrix}_j. \tag{36}$$

Equation (36) presents the relation of in-plane frequency responses at the two ends of the jth straight shaft. Similarly, the relation of out-of-plane frequency responses at the two ends of the jth straight shaft can be expressed in the symbolic vector form as

$$\begin{Bmatrix} \tilde{D}_{l2} \\ \tilde{F}_{l2} \end{Bmatrix}_j = \begin{bmatrix} P_{11} & P_{12} \\ P_{21} & P_{22} \end{bmatrix}_j \begin{Bmatrix} \tilde{D}_{r2} \\ \tilde{F}_{r2} \end{Bmatrix}_j. \tag{37}$$

5. MODAL FREQUENCIES

5.1. FIXED–FIXED CURVED HOLLOW SHAFT

5.1.1. *In-plane motion*

Employing the conditions of zero displacements at two fixed ends of the curved hollow shaft into equation (23) yields the characteristic equation of the curved hollow shaft,

$$[B_{12}]\{F_{l1}\} = \{0\,0\,0\}^{\mathrm{T}}, \tag{38}$$

The ith modal frequency for the in-plane motion of curved hollow shaft satisfies the determinant of $[B_{12}]$ being zero or one eigenvalue of $[B_{12}]$ being zero. Further, the corresponding set of mode shape functions can be obtained by performing similar procedures described by Wang and Sang [7].

5.1.2. *Out-of-plane motion*

The characteristic equation for the out-of-plane motion of the curved hollow shaft with both ends fixed is

$$[C_{12}]\{F_{l2}\} = \{0\,0\,0\}^{\mathrm{T}} \tag{39}$$

from which the ith modal frequency and its corresponding set of mode shape functions can also be obtained by performing similar procedures described by Wang and Sang [7].

5.2. FIXED–FIXED STRAIGHT–CURVED–STRAIGHT HOLLOW SHAFT

5.2.1. *In-plane motion*

The conditions of displacement continuity and force balances at the right conjunction between the curved hollow shaft and the first straight hollow shaft are

$$\{D_{r1}\} = \{\tilde{D}_{l1}\}_1, \{F_{r1}\} = -\{\tilde{F}_{l1}\}_1 \tag{40a}$$

Further, the conditions of displacement continuity and force balances at the left conjunction between the curved shaft and the second straight hollow shaft are

$$\{D_{l1}\} = \{\tilde{D}_{r1}\}_2, \{F_{l1}\} = -\{\tilde{F}_{r1}\}_2 \tag{40b}$$

Substituting equations (40a) and (40b) into equation (23), then employing the relation of responses (36) for $j = 1, 2$ into the result yields the responses relation at the two ends of the whole structure as

$$\begin{Bmatrix} \tilde{D}_{l1} \\ \tilde{F}_{l1} \end{Bmatrix}_2 = \begin{bmatrix} Y_{11} & Y_{12} \\ Y_{21} & Y_{22} \end{bmatrix} \begin{Bmatrix} \tilde{D}_{r1} \\ \tilde{F}_{r1} \end{Bmatrix}_1. \tag{41}$$

where

$$\begin{bmatrix} Y_{11} & Y_{12} \\ Y_{21} & Y_{22} \end{bmatrix} = \begin{bmatrix} H_{11} & H_{12} \\ H_{21} & H_{22} \end{bmatrix}_2 \begin{bmatrix} B_{11} & B_{12} \\ -B_{21} & -B_{22} \end{bmatrix} \begin{bmatrix} H_{11} & H_{12} \\ -H_{21} & -H_{22} \end{bmatrix}_1.$$

Employing the boundary conditions of zero displacements at the two ends of equation (41) yields the characteristic equation for the in-plane motion of the entire structure:

$$[Y_{12}]\{\tilde{F}_{r1}\}_1 = \{0\,0\,0\}^{\mathrm{T}} \tag{42}$$

from which the ith modal frequency and its corresponding set of mode shape functions can also be determined by performing similar procedures described by Wang and Sang [7].

5.2.2. *Out-of-plane motion*

The ith modal frequency and its corresponding set of mode functions for the out-of-plane motion of the entire structure can similarly be determined from the characteristic equation

$$[Z_{12}]\{\tilde{F}_{r2}\}_1 = \{0\,0\,0\}^{\mathrm{T}}, \tag{43}$$

where $[Z_{12}]$ is the sub-matrix of the matrix $[Z]$:

$$[z] = \begin{bmatrix} Z_{11} & Z_{12} \\ Z_{21} & Z_{22} \end{bmatrix} = \begin{bmatrix} P_{11} & P_{12} \\ P_{21} & P_{22} \end{bmatrix}_2 \begin{bmatrix} C_{11} & C_{12} \\ -C_{21} & -C_{22} \end{bmatrix} \begin{bmatrix} P_{11} & P_{12} \\ -P_{21} & -P_{22} \end{bmatrix}_1.$$

6. ORTHOGONALITY

The ith modal frequency and its corresponding displacement components, rotation angle, stress resultants and stress-couple resultant for the in-plane motion of the curved hollow

shaft are denoted as Ω_i, $U_x^{(i)}$, $U_y^{(i)}$, $\Phi_z^{(i)}$, $Q_x^{(i)}$, $Q_y^{(i)}$ and $M_z^{(i)}$ respectively. Further, the ith modal frequency and its corresponding displacement component, rotation angles, stress resultant and stress-couple resultants for the out-of-plane motion of the curved shaft are denoted as ω_i, $U_z^{(i)}$, $\Phi_x^{(i)}$, $\Phi_y^{(i)}$, $Q_z^{(i)}$, $M_x^{(i)}$ and $M_y^{(i)}$ respectively.

6.1. FIXED–FIXED CURVED HOLLOW SHAFT

By performing similar procedures to those described by Wang and Sang [7], the following four equations are obtained:

$$\rho \int_0^L (AU_x^{(i)}U_x^{(k)} + AU_y^{(i)}U_y^{(k)} + I_z\Phi_z^{(i)}\Phi_z^{(k)})\,\mathrm{d}y = 0. \tag{44a}$$

$$\int_0^L \left(\frac{M_z^{(i)}M_z^{(k)}}{EI_z} + \frac{Q_y^{(i)}Q_y^{(k)}}{EA} + \frac{Q_x^{(i)}Q_x^{(k)}}{\kappa GA}\right)\mathrm{d}y = 0, \tag{44b}$$

$$\rho \int_0^L (AU_z^{(i)}U_z^{(k)} + I_x\Phi_x^{(i)}\Phi_x^{(k)} + J\Phi_y^{(i)}\Phi_y^{(k)})\,\mathrm{d}y = 0. \tag{44c}$$

$$\int_0^L \left(\frac{M_x^{(i)}M_x^{(k)}}{EI_x} + \frac{M_y^{(i)}M_y^{(k)}}{GJ} + \frac{Q_z^{(i)}Q_z^{(k)}}{\kappa GA}\right)\mathrm{d}y = 0, \quad i \neq k. \tag{44d}$$

Equations (44a), (44b), (44c) and (44d) indicate that the corresponding sets of mode shape functions of any two distinct modal frequencies for both the in-plane motion and out-of-plane motion of the curved hollow shaft are orthogonal to each other. Further, the following two equations are obtained:

$$\rho\Omega_i^2 \int_0^L (AU_x^{(i)^2} + AU_y^{(i)^2} + I_z\Phi_z^{(i)^2})\,\mathrm{d}y = \int_0^L \left(\frac{M_z^{(i)^2}}{EI_z} + \frac{Q_y^{(i)^2}}{EA} + \frac{Q_x^{(i)^2}}{\kappa GA}\right)\mathrm{d}y, \tag{45a}$$

$$\rho\omega_i^2 \int_0^L (AU_z^{(i)^2} + I_x\Phi_x^{(i)^2} + J\Phi_y^{(i)^2})\,\mathrm{d}y = \int_0^L \left(\frac{M_x^{(i)^2}}{EI_x} + \frac{M_y^{(i)^2}}{GJ} + \frac{Q_z^{(i)^2}}{\kappa GA}\right)\mathrm{d}y. \tag{45b}$$

6.2. STRAIGHT–CURVED–STRAIGHT HOLLOW SHAFT

The orthogonality of two distinct sets of mode shape functions for both the out-of-plane motion and in-plane motion of the entire structure is similarly obtained:

$$\rho \sum_{j=1}^{2} \int_0^{L_j} (A\tilde{U}_{zj}^{(i)}A\tilde{U}_{zj}^{(k)} + J\tilde{\Phi}_{yj}^{(i)}\Phi_{yj}^{(k)} + I_x\tilde{\Phi}_{xj}^{(i)}\Phi_{xj}^{(k)})\,\mathrm{d}y$$

$$+ \rho \int_0^L (A\tilde{U}_z^{(i)}\tilde{U}_z^{(k)} + I_x\Phi_x^{(i)}\Phi_x^{(k)} + J\tilde{\Phi}_y^{(i)}\Phi_y^{(k)})\,\mathrm{d}y = 0. \tag{46a}$$

$$\sum_{j=1}^{2}\int_0^{L_j}\left(\frac{\tilde{Q}_{zj}^{(i)}\tilde{Q}_{zj}^{(k)}}{\kappa GA}+\frac{\tilde{M}_{xj}^{(i)}\tilde{M}_{xj}^{(k)}}{EI}+\frac{\tilde{M}_{yj}^{(i)}\tilde{M}_{yj}^{(k)}}{GJ}\right)\mathrm{d}y$$

$$+\int_0^{L}\left(\frac{Q_z^{(i)}Q_z^{(k)}}{\kappa GA}+\frac{M_x^{(i)}M_x^{(k)}}{EI_x}+\frac{M_y^{(i)}M_y^{(k)}}{GJ}\right)\mathrm{d}y=0,\quad i\neq k. \tag{46b}$$

$$\rho\sum_{j=1}^{2}\int_0^{L_j}(A\tilde{U}_{xj}^{(i)}\tilde{U}_{xj}^{(k)}+A\tilde{U}_{yj}^{(i)}U_{yj}^{(k)}+I_z\tilde{\Phi}_{zj}^{(i)}\tilde{\Phi}_{zj}^{(k)})\,\mathrm{d}y$$

$$+\rho\int_0^{L}(AU_x^{(i)}U_x^{(k)}+AU_y^{(i)}U_y^{(k)}+I_z\Phi_z^{(i)}\Phi_z^{(k)})\,\mathrm{d}y=0. \tag{47a}$$

$$\sum_{j=1}^{2}\int_0^{L_j}\left(\frac{\tilde{Q}_{xj}^{(i)}\tilde{Q}_{xj}^{(k)}}{\kappa GA}+\frac{\tilde{M}_{zj}^{(i)}\tilde{M}_{zj}^{(k)}}{EI_z}+\frac{\tilde{Q}_{yj}^{(i)}\tilde{Q}_{yj}^{(k)}}{EA}\right)\mathrm{d}y$$

$$+\int_0^{L}\left(\frac{Q_x^{(i)}Q_x^{(k)}}{\kappa GA}+\frac{M_z^{(i)}M_z^{(k)}}{EI_z}+\frac{Q_y^{(i)}Q_y^{(k)}}{EA}\right)\mathrm{d}y=0,\quad i\neq k. \tag{47b}$$

Further, the following two equations are obtained:

$$\rho\Omega_i^2\sum_{j=1}^{2}\int_0^{L_j}(A\tilde{U}_{xj}^{(i)^2}+A\tilde{U}_{yj}^{(i)^2}+I_z\tilde{\Phi}_{zj}^{(i)^2})\,\mathrm{d}y+\rho\Omega_i^2\int_0^{L}(AU_x^{(i)^2}+AU_\theta^{(i)^2}+I_z\Phi_z^{(i)^2})\,\mathrm{d}y$$

$$=\sum_{j=1}^{2}\int_0^{L_j}\left(\frac{\tilde{Q}_{xj}^{(i)^2}}{\kappa GA}+\frac{\tilde{Q}_{yj}^{(i)^2}}{EA}+\frac{\tilde{M}_{zj}^{(i)^2}}{EI_z}\right)\mathrm{d}y+\int_0^{L}\left(\frac{Q_x^{(i)^2}}{\kappa GA}+\frac{Q_y^{(i)^2}}{EA}+\frac{M_z^{(i)^2}}{EI_z}\right)\mathrm{d}y. \tag{48a}$$

$$\rho\omega_i^2\sum_{j=1}^{2}\int_0^{L_j}(A\tilde{U}_{zj}^{(i)^2}I_x+\tilde{\Phi}_{xj}^{(i)^2}+J\tilde{\Phi}_{yj}^{(i)^2})\,\mathrm{d}y+\rho\omega_i^2\int_0^{L}(AU_{zj}^{(i)^2}+I_x\Phi_{xj}^{(i)^2}+J\Phi_{yj}^{(i)^2})\,\mathrm{d}y$$

$$=\sum_{j=1}^{2}\int_0^{L_j}\left(\frac{\tilde{Q}_{zj}^{(i)^2}}{\kappa GA}+\frac{\tilde{M}_{xj}^{(i)^2}}{EI_x}+\frac{\tilde{M}_{yj}^{(i)^2}}{GJ}\right)\mathrm{d}y+\int_0^{L}\left(\frac{Q_{zj}^{(i)^2}}{\kappa GA}+\frac{M_{xj}^{(i)^2}}{EI_x}+\frac{M_{yj}^{(i)^2}}{GJ}\right)\mathrm{d}y. \tag{48b}$$

7. EXAMPLES AND DISCUSSION

In most cases, the first modal frequency and its corresponding set of mode shape functions dominate the vibration of structure. Therefore, the effects of initial radius and thickness and radius of cross-section on only the first modal frequency of the two types of hollow shafts are considered in this section. In the method of modal analysis in the numerical computation, the constants $E = 70\,\mathrm{GPa}$, $G = 26\,\mathrm{Gpa}$, $\mu = 0{\cdot}346$. $\rho = 2710\,\mathrm{kg/m^3}$ and the following coefficient κ of the circular hollow shaft [9] are considered:

$$\kappa=\frac{6(1+\mu)(1+m)^2}{(7+6\mu)(1+m)^2+(20+12\mu)m^2} \tag{49}$$

where $m = (a - 0{\cdot}5h)/(a + 0{\cdot}5h)$.

7.1. CURVED HOLLOW SHAFT

The lowest three modal frequencies and their corresponding mode shapes U_x for the in-plane motion of the curved hollow shaft ($a = 20$ cm, $h = 20$ cm, $L = 10$ m, $R = 30$ m) are

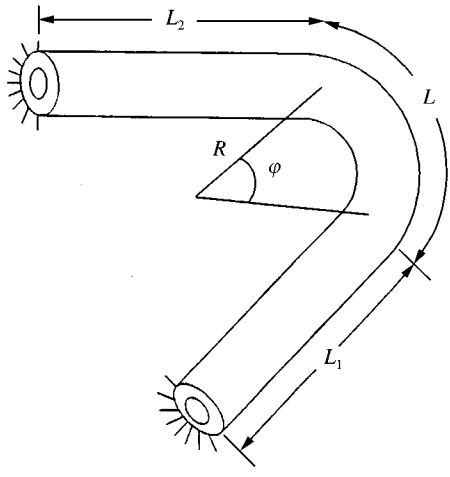

Figure 3. A fixed–fixed straight–curved–straight hollow shaft.

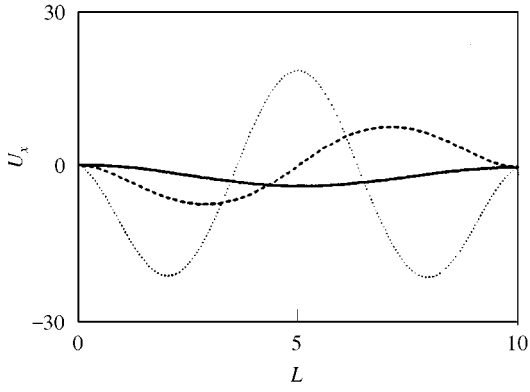

Figure 4. The lowest three modal frequencies and their corresponding mode shapes U_x for the in-plane motion of the curved hollow shaft ($a = 20$ cm, $h = 2$ cm, $L = 10$ m, $R = 30$ m). ——, $\Omega_1 = 261{\cdot}272$ rad/s; – – –, $\Omega_2 = 415{\cdot}003$ rad/s; ⋯, $\Omega_3 = 795{\cdot}871$ rad/s.

displayed in Figure 4. The lowest three modal frequencies and their corresponding mode shapes U_z for the out-of-plane motion of the curved shaft are depicted in Figure 5. Results of the two figures show that these modes are bending modes.

The effect of R on the comparison of Ω_1 and ω_1 of the curved hollow shaft ($a = 20$ cm, $L = 10$ m, $h = 2$ cm is displayed in Figure 6. The initial radius causes a stiffening effect on the in-plane motion. As a result, Ω_1 is greater than ω_1. The stiffening effect decreases as R increases. Therefore, the results of the figure show that the deviation between Ω_1 and ω_1 decreases as R increases. Further, Ω_1 will equal ω_1 as R approaches infinity.

The effect of h on the comparison of Ω_1 and ω_1 of the curved hollow shaft ($a = 20$ cm, $R = 20$ m, $\phi = 30^\circ$) is depicted in Figure 7. The per unit length ratio of bending rigidity (or torsional rigidity) to mass is proportional to the second order of h. Therefore, both Ω_1 and ω_1 are almost linearly proportional to thickness as indicated in the figure. The effect of a on the comparison of Ω_1 and ω_1 of the curved hollow shaft ($h = 2$ cm, $R = 20$ m, $\phi = 30^\circ$) is displayed in Figure 8. The per unit length ratio of bending rigidity (or torsional rigidity) to

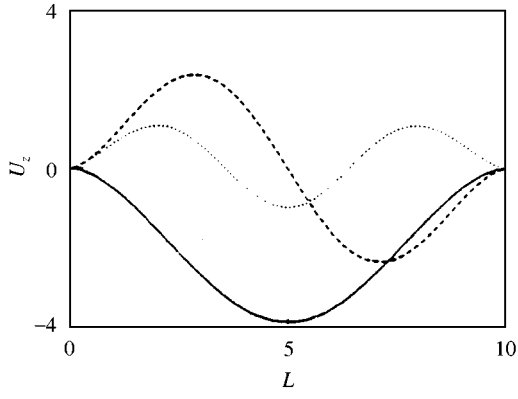

Figure 5. The lowest three modal frequencies and their corresponding mode shapes U_z for the out-of-plane motion of the curved hollow shaft ($a = 20$ cm, $h = 2$ cm, $L = 10$ m, $R = 30$ m). ——, $\omega_1 = 155{\cdot}412$ rad/s; – – –, $\omega_2 = 417{\cdot}631$ rad/s; ····, $\omega_3 = 790{\cdot}250$ rad/s.

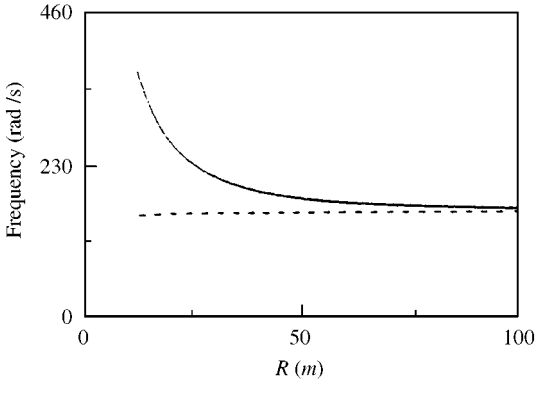

Figure 6. The effect of R on the comparison of Ω_1 and ω_1 of the curved hollow shaft ($a = 20$ cm, $L = 10$ m, $h = 2$ cm): ——, Ω_1; - - - ω_1.

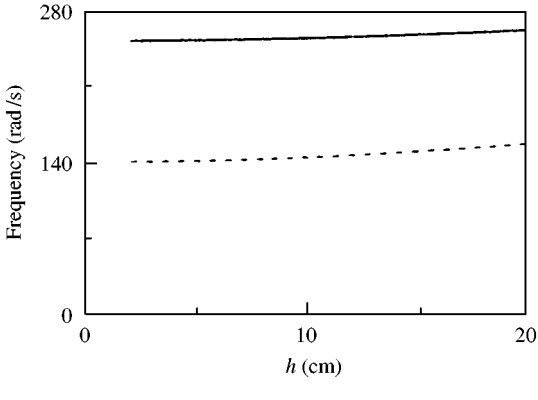

Figure 7. The effect of h on the comparison of Ω_1 and ω_1 of the curved hollow shaft ($a = 20$ cm, $R = 20$ m, $\varphi = 30°$): ——, Ω_1; - - - ω_1.

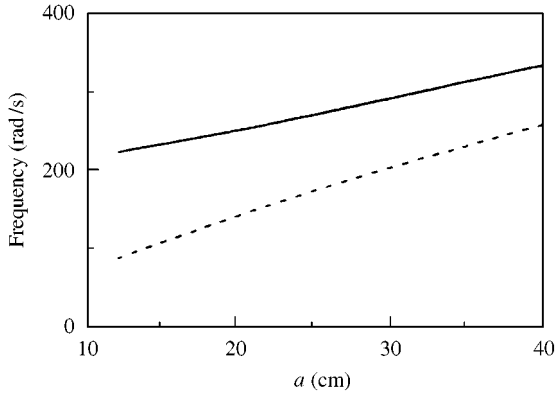

Figure 8. The effect of a on the comparison of Ω_1 and ω_1 of the curved hollow shaft ($h = 2$ cm, $R = 20$ m, $\varphi = 30°$): ——, Ω_1; - - - ω_1.

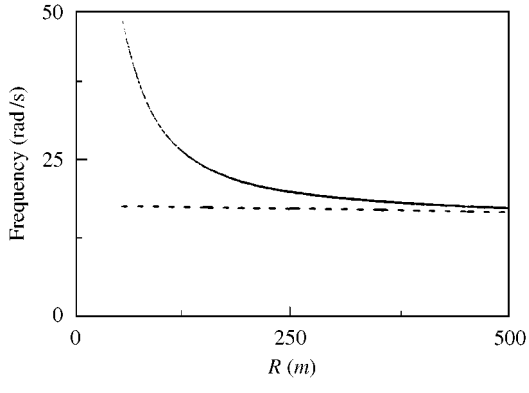

Figure 9. The effect of R on the comparison of Ω_1 and ω_1 of the straight–curved–straight hollow shaft ($a = 20$ cm, $L = 10$ m, $h = 2$ cm): ——, Ω_1; - - - ω_1.

mass is proportional to the second order of a. Therefore, Ω_1 and ω_1 are almost linearly proportional to the radius as indicated in the figure.

7.2. STRAIGHT–CURVED–STRAIGHT HOLLOW SHAFT

The effect of R on the comparison of Ω_1 and ω_1 of the straight–curved–straight hollow shaft ($a = 20$ cm, $L = L_1 = L_2 = 10$ m, $h = 2$ cm) is shown in Figure 9. The initial radius also has a stiffening effect on the in-plane motion. As a result, Ω_1 is greater than ω_1. The stiffening effect decreases as R increases. Therefore, the results of the figure show that the deviation between Ω_1 and ω_1 decreases as R increases. Further, Ω_1 will equal ω_1 as R approaches infinity.

The effect of h on the comparison of Ω_1 and ω_1 of the straight–curved–straight hollow shaft ($a = 20$ cm, $L = 10$ m, $L_1 = L_2 = 10$ m, $R = 20$ m) is shown in Figure 10. The per unit length ratio of bending rigidity (or torsional rigidity) to mass is proportional to the second order of h. Therefore, both Ω_1 and ω_1 are almost linearly proportional to the thickness as indicated in the figure. The effect of a on the comparison of Ω_1 and ω_1 of the straight–curved–straight hollow shaft ($h = 2$ cm, $R = 20$ m, $L = 10$ m, $L_1 = L_2 = 10$ m) is

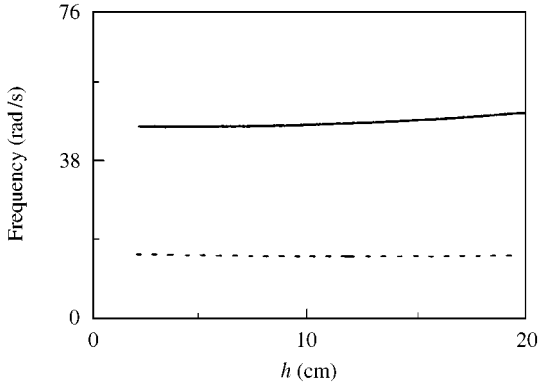

Figure 10. The effect of h on the comparison of Ω_1 and ω_1 of the straight–curved–straight hollow shaft ($a = 20$ cm, $R = 20$ m, $\varphi = 30°$): ——, Ω_1; - - - ω_1.

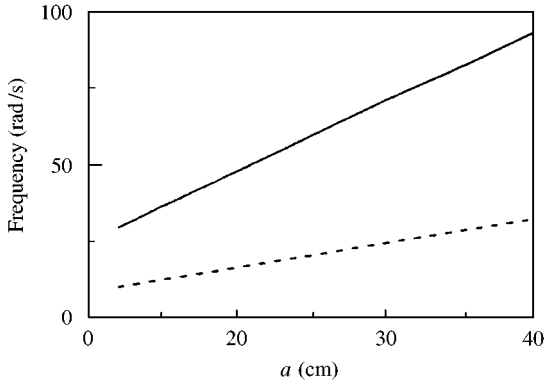

Figure 11. The effect of a on the comparison of Ω_1 and ω_1 of the straight–curved–straight hollow shaft ($h = 2$ cm, $R = 20$ m, $\varphi = 30$): ——, Ω_1; - - - ω_1.

shown in Figure 11. The per unit length ratio of bending rigidity (or torsional rigidity) to mass is proportional to the second order of a. Therefore, the results of the figure also show that both Ω_1 and ω_1 are almost linearly proportional to the radius as indicated in the figure.

8. CONCLUSIONS

This study presents the equations for both the in-plane motion and out-of-plane motion of a curved hollow shaft and a straight–curved–straight hollow shaft. The orthogonality of any two distinct sets of mode shape functions for the in-plane motion or the out-of-plane motion of the structures is shown. The forced vibration of the structures can be further investigated via the present study. The first modal frequency of a straight hollow shaft is the lower bound for that of the in-plane motion, but the upper bound for that of the out-of-plane motion, of the same shaft which is curved. The first modal frequency for both the in-plane motion and out-of-plane motion of the structures is almost linearly proportional to the thickness and the radius of the cross-section.

ACKNOWLEDGMENT

This work was sponsored by the National Science Council, Republic of China, under Contract No. 88-2212-E006-015. The financial support is gratefully acknowledged.

REFERENCES

1. F. M. EL-AMIN and M. A. KASEM 1978 *International Journal for Numerical Methods in Engineering* **12**, 159–167. Higher-order horizontally-curved beam finite element including warping for steel bridges.
2. A. O. LEBECK and J. S. KNOWLTON 1985 *International Journal for Numerical Methods in Engineering* **21**, 421–435. A finite element for three-dimensional deformations of a circular ring.
3. S. S. RAO 1971 *Journal of Sound* **16**, 551–566. Effect of transverse shear and rotatory inertia on the couples twist-bending vibrations of circular rings.
4. T. M. WANG, A. J. LASKEY and M. F. AHMAD 1984 *International Journal of Solids and Structures* **20**, 257–265. Natural frequencies for out-of-plane vibrations of continuous curved beams considering shear and rotatory inertia.
5. J. M. M. SILVA and A. P. V. URGUEIRA 1988 *International Journal of Solids and Structures* **24**, 271–284. Out-of-plane dynamic response of curved beams-an analytical model.
6. V. Z. VLASOV 1961 *Thin Walled Elastic Beams*. Washington, DC: National Science Foundation. Second edition.
7. R. T. WANG and Y. L. SANG 1999 *Structural Engineering and Mechanics, An International Journal* **7**, 361–375. Out-of-plane vibration of multi-span curved beam due to moving loads.
8. R. T. WANG 1998 *Journal of Sound and Vibration* **215**, 143–165. Vibration of a T-type curved frame due to a moving force.
9. C. L. DYM and I. H. SHAMES 1973 *Solid Mechanics: A Variational Approach*. New York: McGraw-Hill.